Accepted for publication in ApJ

A search for broad infrared recombination lines in NGC 1068 [1]

D. Lutz[2], R. Genzel[2], E. Sturm[2], L. Tacconi[2], E. Wieprecht[2], T. Alexander[3], H. Netzer[4], A. Sternberg[4], A.F.M. Moorwood[5], R.A.E. Fosbury[5], K. Fricke[6], S.J. Wagner[7], A. Quirrenbach[8], H. Awaki[9], K.Y. Lo[10]

ABSTRACT

We report infrared spectroscopy of the prototypical Seyfert 2 galaxy NGC 1068, aiming at detection of broad components of hydrogen recombination lines that originate in the obscured broad-line region. Using the Short Wavelength Spectrometer on board the Infrared Space Observatory, we have observed for the first time the regions of Brackett β 2.626μm and Pfund α 7.460μm, and present improved data for Brackett α 4.052μm. No significant broad components are detected, implying an equivalent visual extinction to the broad-line region of at least 50 magnitudes and an obscuring column density of at least 10^{23}cm^{-2}. While consistent with a highly obscured broad-line region, as required by the classical unified scenario, these limits are not yet significant enough to discriminate strongly between different torus models or to constrain properties of the gas causing the very large X-ray obscuration. We discuss the systematic limitations of infrared broad-line region searches and suggest that Brackett α may often be the most favorable transition for future searches.

---

[1]Based on observations with ISO, an ESA project with instruments funded by ESA Member States (especially the PI countries: France, Germany, the Netherlands and the United Kingdom) with the participation of ISAS and NASA.

[2]Max-Planck-Institut für extraterrestrische Physik, Postfach 1603, 85740 Garching, Germany

[3]Institute for Advanced Study, Olden Lane, Princeton, NJ 08540, USA

[4]School of Physics and Astronomy and Wise Observatory, Raymond and Beverly Sackler Faculty of Exact Sciences, Tel Aviv University, Ramat Aviv, Tel Aviv 69978, Israel

[5]European Southern Observatory, Karl-Schwarzschild-Straße 2, 85748 Garching, Germany

[6]Universitätssternwarte Göttingen, Geismarlandstraße 11, 37083 Göttingen, Germany

[7]Landessternwarte, Königstuhl, 69117 Heidelberg, Germany

[8]Center for Astrophysics and Space Sciences, University of California, San Diego, Mail Code 0424, La Jolla, CA 92093-0424,USA

[9]Department of Physics, Faculty of Science, Kyoto University, Sakyo-ku, Kyoto, 606-01, Japan

[10]Institute of Astronomy and Astrophysics, Academia Sinica, Taipei 115, Taiwan, ROC

Subject headings: galaxies: individual (NGC 1068) — galaxies: Seyfert — infrared: ISM: lines and bands

1. Introduction

The prototypical Seyfert 2 galaxy NGC 1068 has played a key role in the development of 'unified' models in which Seyfert 2 galaxies host a Seyfert 1 – like broad-line region (BLR). These models assume that the Seyfert 2 BLR is obscured toward our line of sight by a dusty torus, and have been highly successful in explaining several aspects of Seyfert galaxies. The key observational evidence supporting such models came from the spectropolarimetric dectection of broad hydrogen recombination lines, first in NGC 1068 (Antonucci & Miller 1985) and later in a number of other Seyfert 2s. Direct detection of the obscured BLR may be, in principle, possible at near- and mid-infrared wavelengths and can provide another route to studies of Seyfert unification, independent of the uncertain scattering efficiency entering the quantitative analysis of most spectropolarimetric data. In addition, if good detections or limits could be obtained for a significant sample of Seyfert 2s it would be possible to place constraints on column densities and geometries of the putative tori, by studying detection rates and columns as a function of orientation.

Successes have been reported in detecting broad components of near-infrared recombination lines in several type 2 Seyferts (e.g. Rix et al. 1990; Blanco et al. 1990; Goodrich et al. 1994; Ruiz et al. 1994; Veilleux et al. 1997). However, the observed FWHM line widths (1000 to 3000 km/s) are typically narrower than those of most classical broad-line regions. In NGC 5506, for example, the broadish component may trace an obscured narrow-line region (NLR) component rather than a true dense BLR (Goodrich et al. 1994). In addition, column densities of a few times 10^{22}cm^{-2} as accessible to near-infrared spectroscopy fall short of the column densities expected from pc-scale torus scenarios (Krolik & Begelman 1988), and barely reach column densities directly inferred from mm interferometric observations of near-nuclear gas in NGC 1068 (e.g. Tacconi et al. 1994). Near-IR broad-line detections apparently pick a biased subsample: some of the detections (NGC 2992, NGC 5506, A0945-30), in fact, refer to narrow-line X-ray galaxies, in which the detection of strong X-rays suggests a significantly lower obscuring column than in most classical Seyfert 2s. Some of them had been previously suggested to be intermediate Seyferts on the basis of possible broad lines in their optical spectra.

X-ray observations are, by far, the most sensitive large column density indicators. The measured obscuring columns in Seyfert 2 galaxies range from few $\times\,10^{20}$ cm^{-2} to $>10^{25}$ cm^{-2} (e.g. Turner et al. 1997; Bassani et al. 1999) suggesting that near-infrared lines may be usually fully absorbed. However, the relation between X-ray column and infrared obscuration may depend on properties of the obscuring material. There is, hence, a strong rationale for trying to detect longer wavelength recombination lines that are capable of penetrating a larger column, and to extend searches to more difficult but more rewarding X-ray quiet targets. In the following, we report on upper limits for broad 2.62μm Brackett β, 4.05μm Brackett α and 7.46μm Pfund α emission from the nuclear region of NGC 1068 which has one of the largest X-ray columns.

The major observational difficulties in attempts to detect broad mid-infrared recombination lines are (1) the rapid fall of intrinsic recombination line fluxes towards higher series, i.e. longer wavelengths; (2) the active galactic nucleus (AGN) dust continuum rising steeply towards longer wavelengths, leading to small line-to-continuum ratios vulnerable to systematic effects; and (3) the shape of the mid-infrared extinction curve which determines the wavelengths capable of penetrating the highest obscuring column. For a galactic type extinction law (e.g. Draine 1989), the Pfund α 7.46μm line might be a 'sweet spot' in being intrinsically still quite bright but suffering little obscuration in the deep extinction minimum near 7μm before the onset of silicate absorption. The same low extinction, able to penetrate columns of $\gtrsim 10^{23}$cm^{-3}, is only found again at very long wavelengths $\gtrsim$30μm where the recombination lines are intrinsically very faint and exceedingly difficult to detect against the strong dust continuum.

2. Observations and limits on emission from the hidden BLR

We have used the Short Wavelength Spectrometer SWS (de Graauw et al. 1996) on board the Infrared Space Observatory ISO (Kessler et al. 1996) to search for broad hydrogen recombination lines in NGC 1068. The observations were targeted at Brackett β 2.62μm, Brackett α 4.05μm and Pfund α 7.46μm, using the SWS06 mode to cover ranges of $\sim$6000km/s (Brackett α which is close to an SWS 'band edge', see below) to $\sim$14000km/s (Pfund α) at a good signal-to-noise ratio. The $14'' \times 20''$ aperture was oriented approximately north-south and centered on the nucleus, thus covering any hidden BLR, the NLR and part of the extended emission line region. Humphreys α (n=7-6) 12.37μm was observed as well but does not provide a useful measurement since the SWS relative spectral response in this wavelength range is less well defined due to a very complex fringing pattern. We have analyzed the data using the SWS Interactive Analysis (IA) system (Lahuis et al. 1998; Wieprecht et al. 1998) and calibration files as of July 1998. A more detailed discussion of the data analysis is given by Lutz et al. (2000) together with a presentation of our complete SWS dataset on NGC 1068.

Broad emission is not detected significantly in any of the three lines. We will now discuss the upper limits on broad components of the various lines (Table 1), adopting $\sim$3000km/s as the FHWM of the broad emission. This is the FHWM measured for NGC 1068 in polarized Hβ (Miller et al. 1991, Inglis et al. 1995) from regions where linewidth-preserving dust scattering dominates the scattering process. Particular attention is given to the effects of relative spectral response calibration and of broad emission features from complex molecules in the ISM on the determination of the underlying continuum. These are limiting factors in the search for the BLR in the strong near- to mid-infrared continuum of NGC 1068.

At Brackett β, NLR emission is clearly seen (Figure 1). Lutz et al. (2000) find NLR fine structure lines over a wide range of conditions reasonably well fitted by a profile with two gaussian components, having FWHM 333 and 1246 km/s, peak ratio narrow/wide 1.34, and the wider component blueshifted by 100km/s. This is consistent with the Brackett β profile within the (considerable) noise. Brackett β is blended with the (1-0) O(2) ro-vibrational transition of molecular hydrogen. Based on other observed H_2 lines (Lutz et al. 2000), this transition is, however, estimated to be a minor contributor ($\lesssim$10%) to the flux for the case of NGC 1068. Our limit on broad (FWHM 3000 km/s) emission is mainly set by noise despite an integration time of $\approx$3 hours. The line is observed close to the edge of one of the SWS 'AOT bands' (de Graauw et al. 1996) . This implies increased uncertainties in the relative spectral response calibration compared to the band centers, but there is no manifest effect on the Brackett β data, since the variation of sensitivity with wavelength is slow for this particular band limit. Some of the large scale curvature in the Brackett β spectrum may be due to this effect. The curvature almost certainly does not suggest an extremely broad BLR component and would be inconsistent with the spectropolarimetric evidence on the width of BLR lines. We note that the S/N of the data approaches the limit given by the (average) noise in the relative spectral response function of the twelve detectors at this wavelength.

For Brackett α, the relative spectral response changes by a factor of almost two over the short range covered by the line (Figure 2) which is at the long wavelength end of the SWS AOT band 1E. Under these conditions, systematic effects are very important in addition to the (low) detector noise. There may be residual systematic uncertainties in the spline smoothing process used for in-orbit calibration of the SWS relative spectral response (B. Vandenbussche, priv. comm.). Also, small inaccuracies of dark current subtraction can imprint a residue of the relative spectral response function on the final spectrum. The wavelength range above 4.08μm was observed as well, but is not shown since it does not contribute to the Brackett α profile because of much higher detector noise. When overplotting the Brackett α profile with the NLR profile which fits the observed fine structure lines quite well (Fig. 2), or attempting fits of two gaussians on a sloped continuum, the wings of the Brackett α profile appear slightly wider than for the typical NLR profile. We do not consider this a detection of a broad component, however, because the excess would be $\lesssim$1% of the continuum and not fully robust with respect to the mentioned spectral response calibration uncertainties and to location of the continuum. In Table 1 we quote a conservative upper limit for a broad component, estimated on the basis of possible systematic problems. The nondetection of broad Brackett α strengthens previous limits on such a component (DePoy 1987; Oliva & Moorwood 1990).

Figure 3 shows the result of an $\sim$1 hour integration on the Pfund α region. In this high S/N spectrum we see the wing of the very strong [Ne VI] line as well as faint [Na III] 7.318μm and a possible unidentified feature at rest wavelength $\sim$7.555μm. Pfund α is not clearly detected, although there is a marginally significant maximum at the expected redshift (observed wavelength 7.489μm) and strength of NLR Pfund α, as predicted from NLR Brackett α, case B ratios, and assuming low NLR extinction. Again, we have set a conservative limit on a possible broad-line region contribution to Pfund α. The main limitation of Pfund α BLR searches is the continuum definition rather than the signal-to-noise ratio of the line: not only are there the interfering lines of [Ne VI] and [Na III] but also, more importantly, the effect of continuum features. This is better illustrated in Figure 4 which shows a larger part of the full SWS spectrum of NGC 1068 (Lutz et al. 2000) around Pfund α both as observed, and with a tentative addition of faint starburst activity (taken from a scaled spectrum of M 82) to the spectrum of NGC 1068 dominated by NLR dust. It is obvious that the starburst-related emission features usually ascribed to polycyclic aromatic hydrocarbons (PAHs) will induce curvature of the 'continuum' near Pfund α since this is where the main '7.7μm' PAH feature starts to rise. This curvature will make detection of very broad lines difficult if there is significant circumnuclear star formation. In addition, the shapes of the PAH features are known to vary in detail with local conditions (e.g. Verstraete et al. 1996; Roelfsema et al. 1996). While they are likely destroyed very close to the central AGN, regions further out may contribute to a spectrum like that of NGC 1068 with PAH shapes differing from those for a canonical starburst, making accurate correction difficult. Similar continuum definition problems may arise at a lower level even if there is no active circumnuclear starburst, since PAH emission will be widespread also in the more quiescent disk of the Seyfert host (e.g. Mattila et al. 1999).

3. Discussion

What are the implications of our upper limits on broad lines for the structure of the obscuring material? The derived obscuring column density sensitively depends on the adopted intrinsic BLR line fluxes which are usually not known accurately. For the favorable case of NGC 1068, we are able to derive estimates (Table 1) on the basis of the intrinsic broad Hβ flux derived from spectropolarimetry (Miller et al. 1991; Inglis et al. 1995), and of case B recombination line ratios. Case B is not strictly adequate for BLR conditions since large optical depths are expected in the Balmer and Paschen lines (e.g. Netzer 1990 and references therein). However, except for the leading line in each series, the IR to optical line ratios are not expected to deviate much from this simple approximation and we have therefore adopted the calculations by Storey & Hummer (1995) as our best estimates. The ratios are not sensitive to the adopted density and temperature and we have used the $T_e = 10000$K, $n_e = 10^6$cm^{-3} values computed from their code. The ratios relative to Hβ are therefore 0.0426 for Brackett β, 0.0725 for Brackett α, and 0.0224 for Pfund α.

We adopt an intrinsic broad Hβ flux of $\sim 1 \times 10^{-17}$W cm^{-2} on the basis of the reassuringly consistent spectropolarimetric estimates of Miller, Goodrich, & Matthews (1991) and Inglis et al. (1995). Inglis et al. estimate an intrinsic broad Hα flux of 4.3×10^{-17}W cm^{-2}, consistent with our value for a typical Balmer decrement observed in AGN ($\simeq 4$). The intrinsic broad Hβ flux of 2.48×10^{-18}W cm^{-2} quoted by Miller, Goodrich, & Matthews (1991) has to be corrected upwards for our purposes: it is derived from the *observed* total narrow [O III] 5007Å flux (Shields & Oke 1975) and the broad Hβ / narrow [O III] ratio in scattered light, taken from the 'NE knot' where the scattering properties are most homogeneous. The extinction to the narrow-line region of NGC 1068 is, however, known to be significant at the wavelength of [O III] 5007Å. We correct to our intrinsic broad Hβ flux of 1×10^{-17}W cm^{-2}, using an [O III] 5007Å correction factor of $\sim$4 consistent with the available extinction studies (Neugebauer et al. 1980; Koski 1978; Ward et al. 1987). The spectropolarimetric estimates for the intrinsic BLR flux implicitly assume that the scatterers in the 'NE knot' have a similarly unobscured view of the BLR *and* NLR.

It is evident from Table 1 that the limits measured by ISO imply a significant obscuration of the BLR in the infrared. Independent of detailed flux estimates, this can be explained by the following simple argument: intrinsically, the broad component of Hβ will dominate the total Hβ flux. This is typical for Seyferts 1 in general, but for NGC 1068 also demonstrated directly by spectropolarimetry (Miller et al. 1991; Inglis et al. 1995). Then, if an observation detects a NLR recombination line at good S/N but fails to detect its broad component, the additional BLR obscuration at that wavelength must (still) be significant.

A Brackett α obscuration of >2.4 mag (Table 1) corresponds to an equivalent visual obscuration of A$_V$ $\gtrsim$50 mag, and an obscuring column density of more than $\approx 10^{23}$cm^{-2}. These quantities depend somewhat on the adopted extinction curve (cf. Table 1) and on conversion to column density (e.g. for normal ISM conditions and dust-to-gas ratio N$_H$=A$_V$ $\times$ 1.79×10^{21}cm^{-2}, Predehl & Schmitt 1995). A$_V$ $\gtrsim$50 mag is a lower limit using the most conservative assumption of a Galactic center extinction curve with relatively high extinction in the 4-8μm range. If broad Brackett α were detected in our data, it could not be obscured by significantly more than 10^{23}cm^{-2}. This is well below the $\gtrsim$$10^{24}$cm^{-2} columns needed to fit the X-ray properties of Compton-thick Seyferts, which consequently are also the columns used by standard 'compact' torus models (Krolik & Begelman 1988). For NGC 1068, X-ray spectra clearly indicate an even higher obscuring column (e.g. Marshall et al. 1993; Matt et al. 1997). We note however that high columns derived from X-ray spectra do not enforce a priori unobservability of the mid-infrared transitions. The relation between X-ray based column and infrared extinction may vary with gas-to-dust ratio or dust properties of the obscuring gas. Empirically, the relationship between broad-line region optical/infrared obscuration and X-ray absorbing column may vary considerably from source to source (see e.g. cases discussed in Granato et al. 1997; Maiolino et al., in prep). Detections or limits on infrared broad lines could, hence, determine the properties of the putative torus in a way that is independent from X-ray spectroscopy. They could also discriminate among the different classes of torus models, in particular the very high A$_V$ compact ones (e.g Krolik & Begelman 1988; Pier & Krolik 1992) from lower A$_V$ ones where much of the X-ray obscuration will occur in dust-free gas (e.g. Granato & Danese 1994). At this point, the limit of A$_V$ $\gtrsim$50 approaches column densities predicted by some large scale torus models (A$_V$ $\sim$ 72 for NGC 1068, Granato et al. 1997) but is not sufficient to discriminate strongly between the different scenarios. It is however fully consistent with the presence of large molecular column densities inferred from millimeter interferometry (e.g. Tacconi et al. 1994).

Our observations help to shed light on strategies for future infrared BLR searches. If the extinction in the 2-8μm range follows one of the classical curves e.g. the $\lambda^{-1.75}$ power law of Draine (1989), then Pfund α would be the most favorable line for penetrating the highest columns. For such an extinction curve in conjunction with observations limited by instrumental sensitivity, lower extinction compensates for the weaker intrinsic strength of Pfund α. There are, however, indications from ISO spectroscopy that the extinction at Pfund α may be almost as large as at Brackett α (Lutz et al. 1996, Lutz et al. 1997). This value was derived mainly for the line of sight towards our Galactic center, where local conditions could obviously be different from an AGN torus. Other disadvantages of Pfund α are the lower line-to-continuum ratio (for NGC 1068 the continuum rises by a factor of $\sim$2.5 from 4 to 7.5μm), the crowded spectral region with nearby fine structure lines, strong PAH emission features, and the possibility that absorption features similar to those seen towards the Galactic center (Lutz et al. 1996) may be present depending on the physical conditions of the absorber. When using NGC 1068 as a template for future searches for broad Pfund α, two peculiarities should be kept in mind. (1) At all near- and mid-infrared wavelengths, NGC 1068 is known for its strong dust continuum and resulting unusually low NLR line-to-continuum ratios. This should increase the prospects of BLR detection in other Seyfert 2s with more favorable line-to-continuum ratios. (2) On the other hand, the proximity of NGC 1068 minimizes contamination by PAH emission since most of the circumnuclear star formation occurs outside a nuclear aperture, even if it is as large as that of ISO. PAH contamination will be a problem for many other Seyfert 2s (Clavel et al. 1998), even if somewhat smaller apertures can be employed. We hence suggest Brackett α to be a more promising target for infrared BLR searches, being brighter and on a weaker continuum free of strong nearby emission and absorption features. Attempts to detect broad Pfund α will definitely have to use as small as possible apertures to minimize PAH dilution from circumnuclear star formation.

We thank Roberto Maiolino for discussions. SWS and the ISO Spectrometer Data Center at MPE are supported by DLR (DARA) under grants 50 QI 8610 8 and 50 QI 9402 3. We acknowledge support by the German-Israeli Foundation. Astronomical Research at Tel Aviv university is supported in part by the Israeli Science Foundation.

REFERENCES

Alexander T., Sturm E., Lutz D., Sternberg A., Netzer H., Genzel R. 1999, ApJ, 512, 204

Antonucci R.R.J., Miller J.S. 1985, ApJ, 297, 621

Bassani L., Dadina M., Maiolino R., Salvati M., Risaliti G., Della Ceca R., Matt G., Zamorani G. 1999, ApJS, 121, 473

Blanco P.R., Ward M.J., Wright G.S. 1990, MNRAS, 242, 4p

Clavel J., et al. 1998, astro-ph/9806054

DePoy D.L. 1987, in Infrared Astronomy with Arrays, ed. C.G. Wynn-Williams, E.E. Becklin, & L.H. Good (Honolulu: University of Hawaii), 426

Draine B.T. 1989, in: "Proc. 22nd Eslab Symposium on Infrared Spectroscopy in Astronomy", ESA SP-290, (Noordwijk: ESA), 93

Genzel R., et al. 1998, ApJ, 498, 579

Goodrich R.W., Veilleux S., Hill G.J. 1994, ApJ, 422, 521

Granato G.L., Danese L. 1994, MNRAS, 268, 235

Granato G.L., Danese L., Franceschini A. 1997, ApJ, 486, 147

de Graauw Th., et al. 1996, A&A, 315, L49

Inglis M.D., Young S., Hough J.H., Gledhill T., Axon D.J., Bailey J.A., Ward M.J. 1995, MNRAS, 275, 398

Kessler M.F., et al. 1996, A&A, 315, L27

Koski A.T. 1978, ApJ, 223, 56

Krolik J.H., Begelman M.C. 1988, ApJ, 329, 702

Lahuis F., et al. 1998, in Astronomical Data Analysis Software and Systems VII, A.S.P. Conference Series, Vol. 145, eds. R. Albrecht, R.N. Hook and H.A. Bushouse, p.224

Lutz D., et al. 1996, A&A, 315, L269

Lutz D., et al. 1997, in: "First ISO Workshop on Analytical Spectroscopy", eds. A.M. Heras et al., ESA-SP419 (Noordwijk:ESA), 143

Lutz D., Sturm E., Genzel R., Moorwood A.F.M., Alexander T., Nezter H., Sternberg A., 2000, submitted to ApJ

Marshall F.E., et al. 1993, ApJ, 405, 168

Matt G., et al. 1997, A&A, 325, L13

Mattila K., Lehtinen K., Lemke D. 1999, A&A, 342, 643

Miller J.S., Goodrich R.W., Mathews W.G. 1991, ApJ, 378, 1991

Netzer H. 1990, in: Blandford R.D., Netzer H., Woltjer L., "Active Galactic Nuclei", Saas-Fee advanced course 20 (Berlin: Springer), 57

Neugebauer G., et al. 1980, ApJ, 238, 502

Oliva E., Moorwood A.F.M. 1990, ApJ, 348, L5

Pier E.A., Krolik J.H. 1992, ApJ, 401, 99

Predehl P., Schmitt J.H.M.M. 1995, A&A, 293, 889

Rix H.-W., Carleton N.P., Rieke G., Rieke M. 1990, ApJ, 363, 480

Ruiz M., Rieke G.H., Schmidt G.D. 1994, ApJ, 423, 608

Roelfsema P.R., et al. 1996, A&A, 315, L289

Shields G.A., Oke J.B. 1975, ApJ, 197, 5

Storey P.J., Hummer D.G. 1995, MNRAS, 272, 41

Tacconi L.J., Genzel R., Blietz M., Cameron M., Harris A.I., Madden S. 1994, ApJ, 426, L77

Turner T.J., George I.M., Nandra K.M, Mushotzky R.F. 1997, ApJS, 113, 23

Veilleux S., Goodrich R.W., Hill G.J. 1997, ApJ, 477, 631

Verstraete L., Puget J.L., Falgarone E., Drapatz S., Wright C.M., Timmermann R. 1996, A&A, 315, L337

Ward M.J., Geballe T., Smith M., Wade R., Willams P. 1987, ApJ, 316, 138

Wieprecht E., et al. 1998, in Astronomical Data Analysis Software and Systems VII, A.S.P. Conference Series, Vol. 145, eds. R. Albrecht, R.N. Hook and H.A. Bushouse, p.279

Table 1: Limits on broad-line region emission

Line	Wavelength	Observed Flux[a]	Intrinsic flux[b]	A_V[c]	A_V[d]
	μm	$10^{-20}\,\mathrm{W\,cm^{-2}}$	$10^{-20}\,\mathrm{W\,cm^{-2}}$	mag	mag
Brackett β	2.626	< 9	43	>23	>23
Brackett α	4.052	< 8	73	>68	>47
Pfund α	7.460	< 13	23	>52	>14

[a] Upper limits for a broad component with FWHM 3000km/s.

[b] Intrinsic broad-line flux estimates derived for comparison from the unobscured broad Hβ flux estimate of $1 \times 10^{-17}\,\mathrm{W\,cm^{-2}}$ (see text), no extinction, and case B recombination line ratios (Storey & Hummer 1995).

[c] Equivalent visual extinction to the broad-line region, adopting $A_{Br\beta}/A_V = 0.075$, $A_{Br\alpha}/A_V = 0.035$, $A_{Pf\alpha}/A_V = 0.012$ derived from the $\lambda^{-1.75}$ infrared extinction curve of Draine (1989) and $A_V = 5.9 \times E(J-K)$.

[d] Equivalent visual extinction to the broad-line region, adopting $A_{Br\beta}/A_V = 0.075$, $A_{Br\alpha}/A_V = 0.51$, $A_{Pf\alpha}/A_V = 0.44$ representing the extinction curve towards the center of our galaxy (Lutz et al. 1997)

Fig. 1.— Upper panel: Spectrum of the 2.626μm Brackett β line in NGC 1068. The dotted line indicates the suggested upper limit on a FWHM 3000km/s broad-line region component. Lower panel: The structure of the SWS relative spectral response function is shown for one of the detectors used. There is only moderate large scale structure despite the line being close to the edges of one of the SWS 'AOT bands'. The high frequency modulation is detector noise from the calibration used to derive the relative spectral response function.

Fig. 2.— As in Figure 1, for the 4.052μm Brackett α line. Again, the dotted line indicates the suggested upper limit on a FWHM 3000km/s broad-line region component. The lower dashed line represents the larger range continuum slope seen at 3.7 to 4.05μm in the full SWS spectrum (Lutz et al. 2000), offset for clarity. The upper dashed line shows a continuum with the same slope plus a suitably scaled narrow line region profile, as derived by Alexander et al. (2000) from mid-infrared fine structure lines. Note the strong variation of the relative spectral response over the short range covered by the line. Some fringing is seen in the relative spectral response.

Fig. 3.— As in Figure 1, for the 7.460μm Pfund α line. Lines of [Na III] and [Ne VI] are observed in this range, as well as a possible unidentified feature. Again, the relative spectral response shows fringes.

Fig. 4.— The effect of PAH emission due to starburst activity on the detectability of broad Pfund α 7.46μm emission. Part of the full SWS spectrum of NGC 1068 is shown, slightly smoothed to suppress noise. The dotted line shows the same spectrum, after adding a redshifted and arbitrarily scaled version of the spectrum of the starburst M82 intended to show the effect of additional weak starburst activity. For clarity, emission lines have been omitted from the M82 spectrum. The addition of PAH features introduces curvature to the 'continuum' at the location of Pfund α 7.46μm.

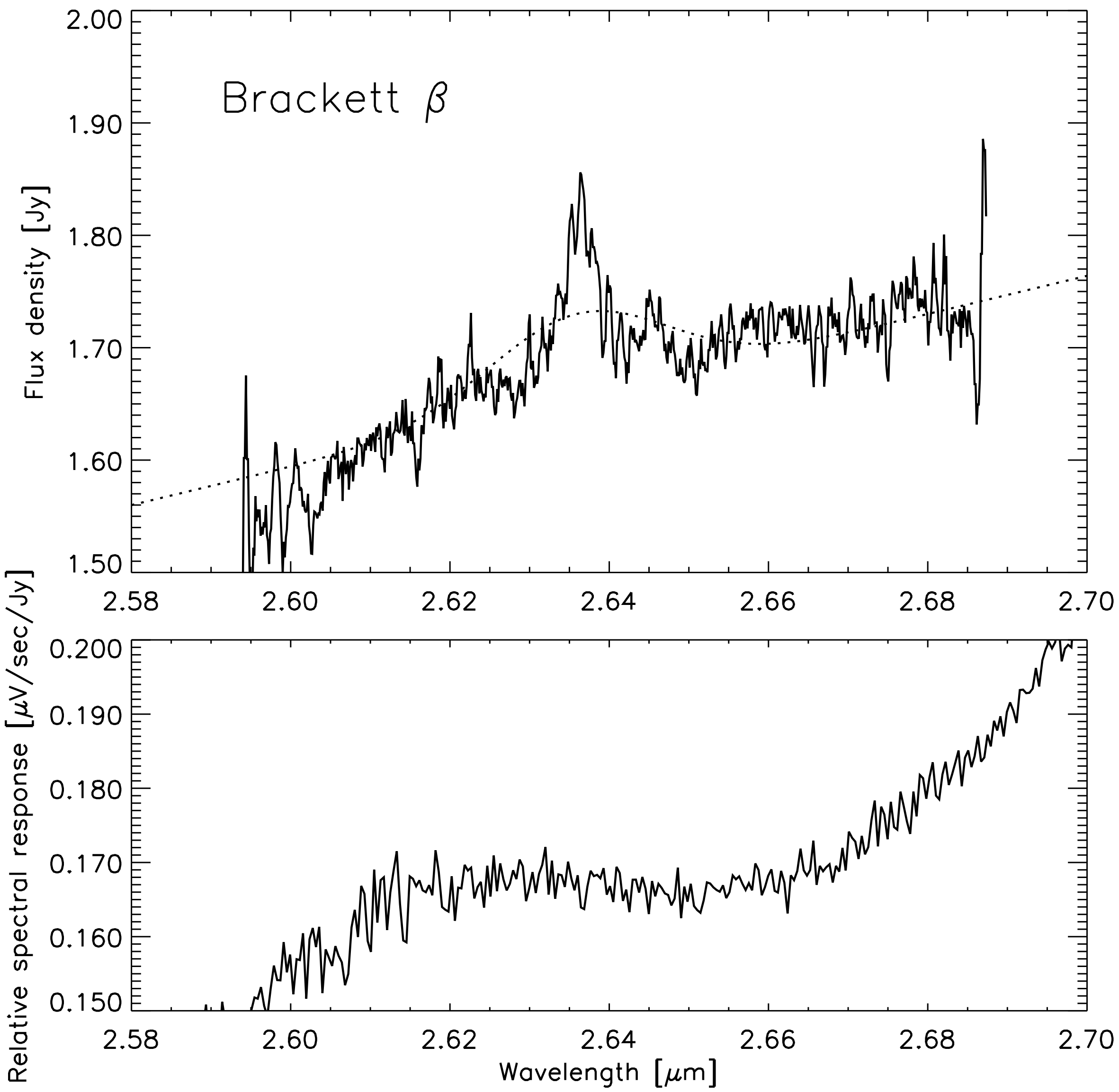
Brackett β
Flux density [Jy]
2.00
1.90
1.80
1.70
1.60
1.50
2.58
2.60
2.62
2.64
2.66
2.68
2.70
Relative spectral response [μV/sec/Jy]
0.200
0.190
0.180
0.170
0.160
0.150
2.58
2.60
2.62
2.64
2.66
2.68
2.70
Wavelength [μm]

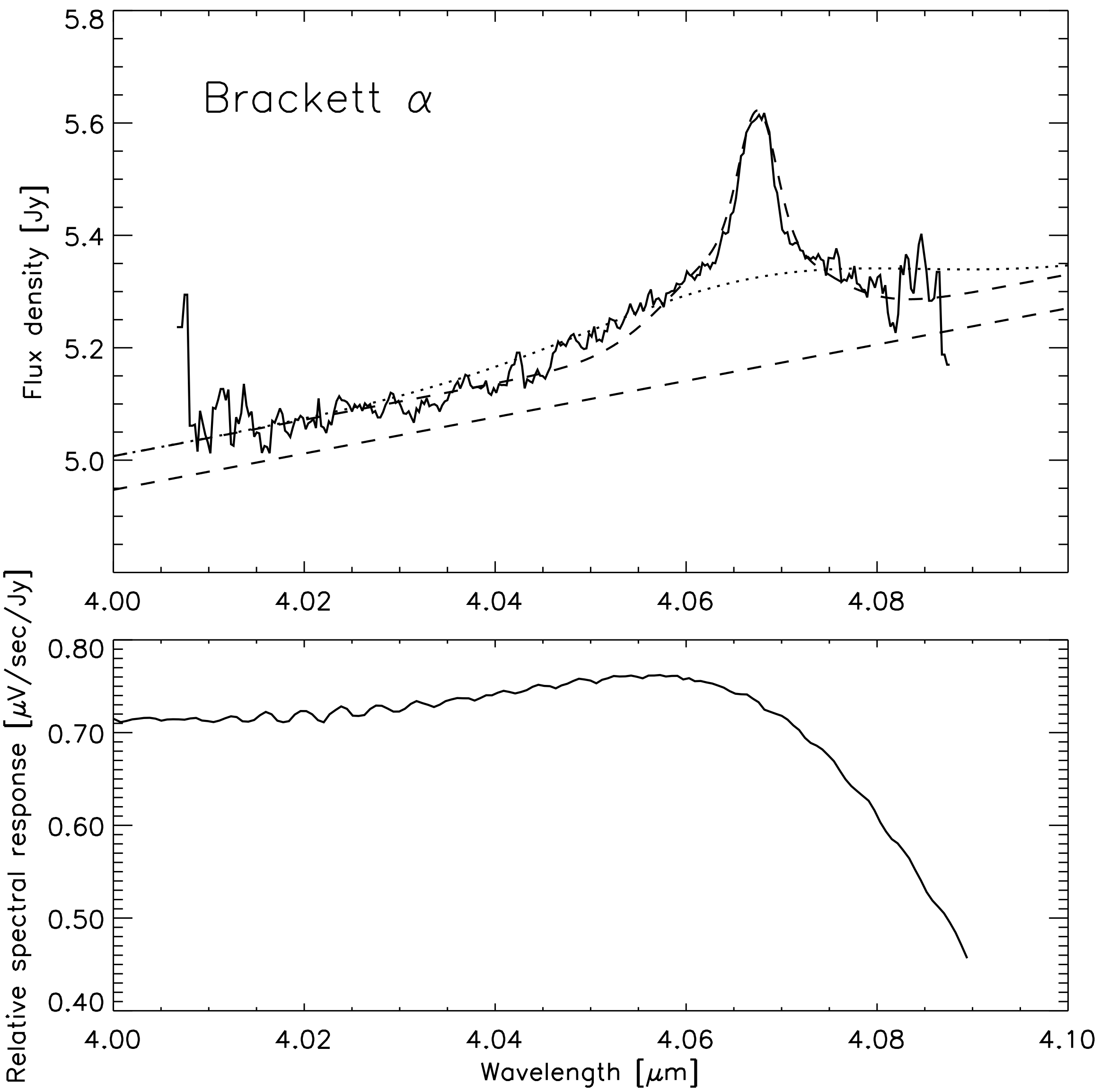
Brackett α
Flux density [Jy]
5.8
5.6
5.4
5.2
5.0
4.00
4.02
4.04
4.06
4.08
Relative spectral response [μV/sec/Jy]
0.80
0.70
0.60
0.50
0.40
4.00
4.02
4.04
4.06
4.08
4.10
Wavelength [μm]

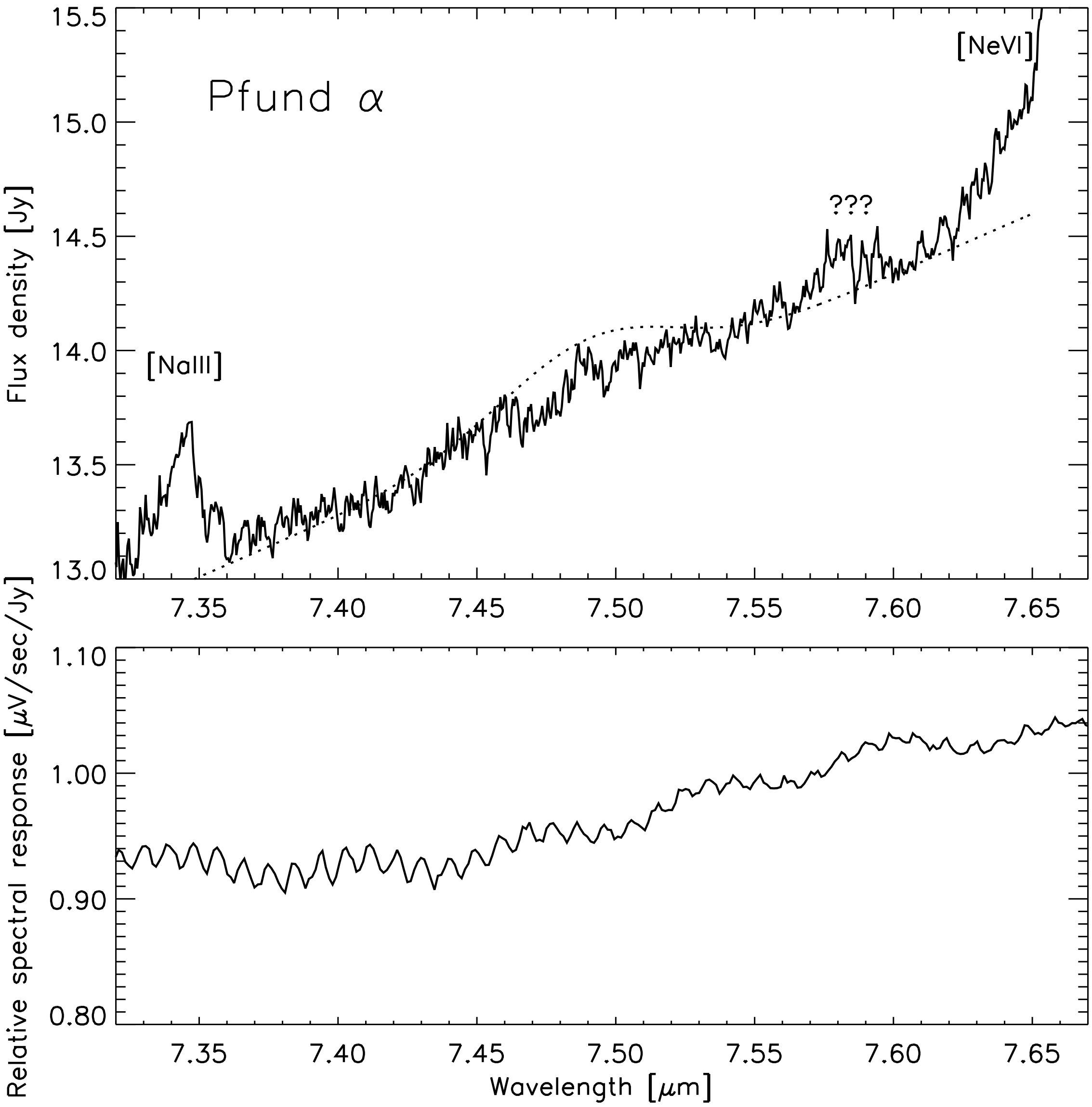
Pfund α
[NaIII]
???
[NeVI]
Flux density [Jy]
15.5
15.0
14.5
14.0
13.5
13.0
7.35
7.40
7.45
7.50
7.55
7.60
7.65
Relative spectral response [μV/sec/Jy]
1.10
1.00
0.90
0.80
Wavelength [μm]

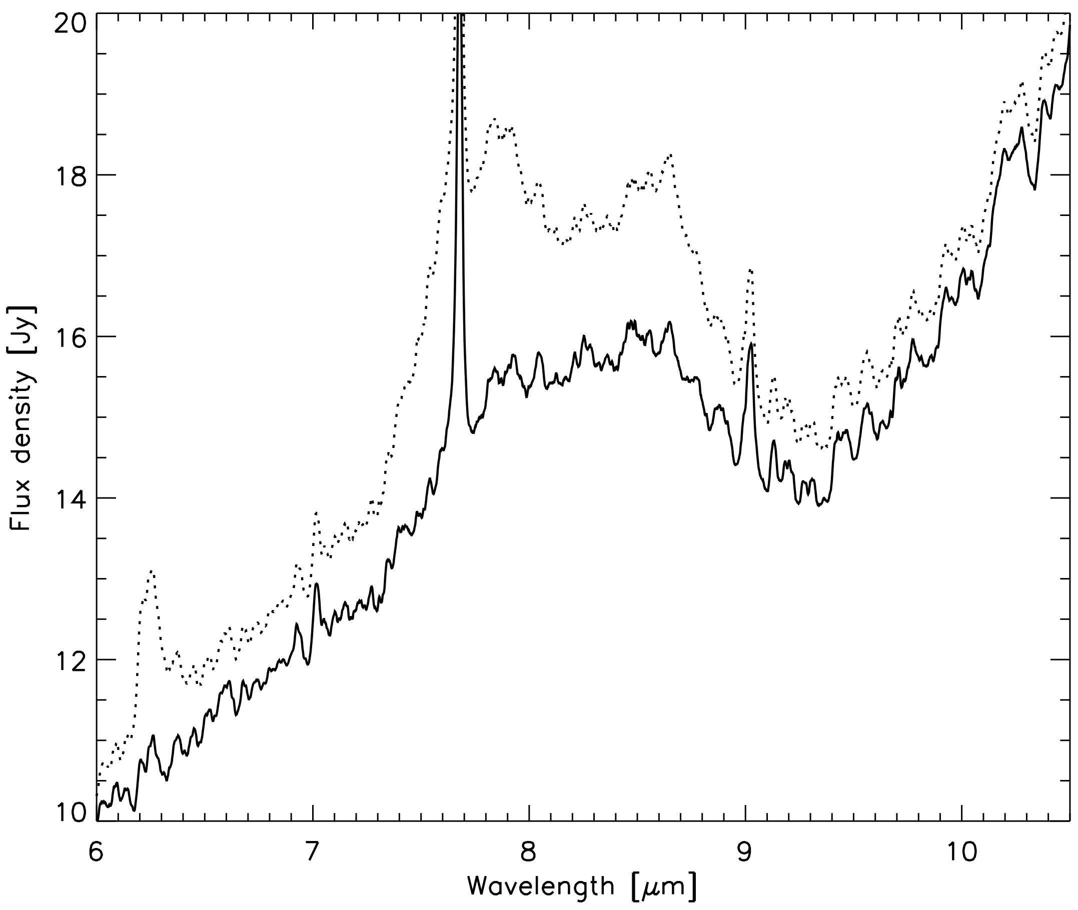
20
18
16
14
12
10
Flux density [Jy]
6
7
8
9
10
Wavelength [μm]